Overview of Aircraft Observations in Emerging Science in MJO

Shuyi S. Chen, Brandon Kerns, Chiaying Lee and Falko Judt
RSMAS/University of Miami
David Jorgensen and Nick Guy
NSSL/NOAA
Julien Delanoë, Nicolas Viltard, and Emmanuel Fontaine
LATMOS-Institute Pierre Simon Laplace, France
Chris Zappa
University of Columbia

(AGU Fall Meeting, 3 December 2012, San Francisco)

Aircraft Observations in DYNAMO and Relevance to MJO

Main objectives:

- Convection-environment interactions in MJO
- Full 3-D structure of convective cloud systems
- Ice microphysical properties of convective cloud systems
- Large-scale atmospheric water vapor and upper ocean variability
- Air-sea fluxes and boundary layer structure

Key results:

1) Sampling in suppressed, transition, and active phases of MJO
2) Large-scale atmospheric moisture, temperature, wind, and upper ocean observations using dropsondes and AXBTs
3) P-3 and Falcon aircraft multi-radar (C-band, W-band) observations of 3-D structure of convective cloud systems
4) Convective cold pool structure and recovery in MJO

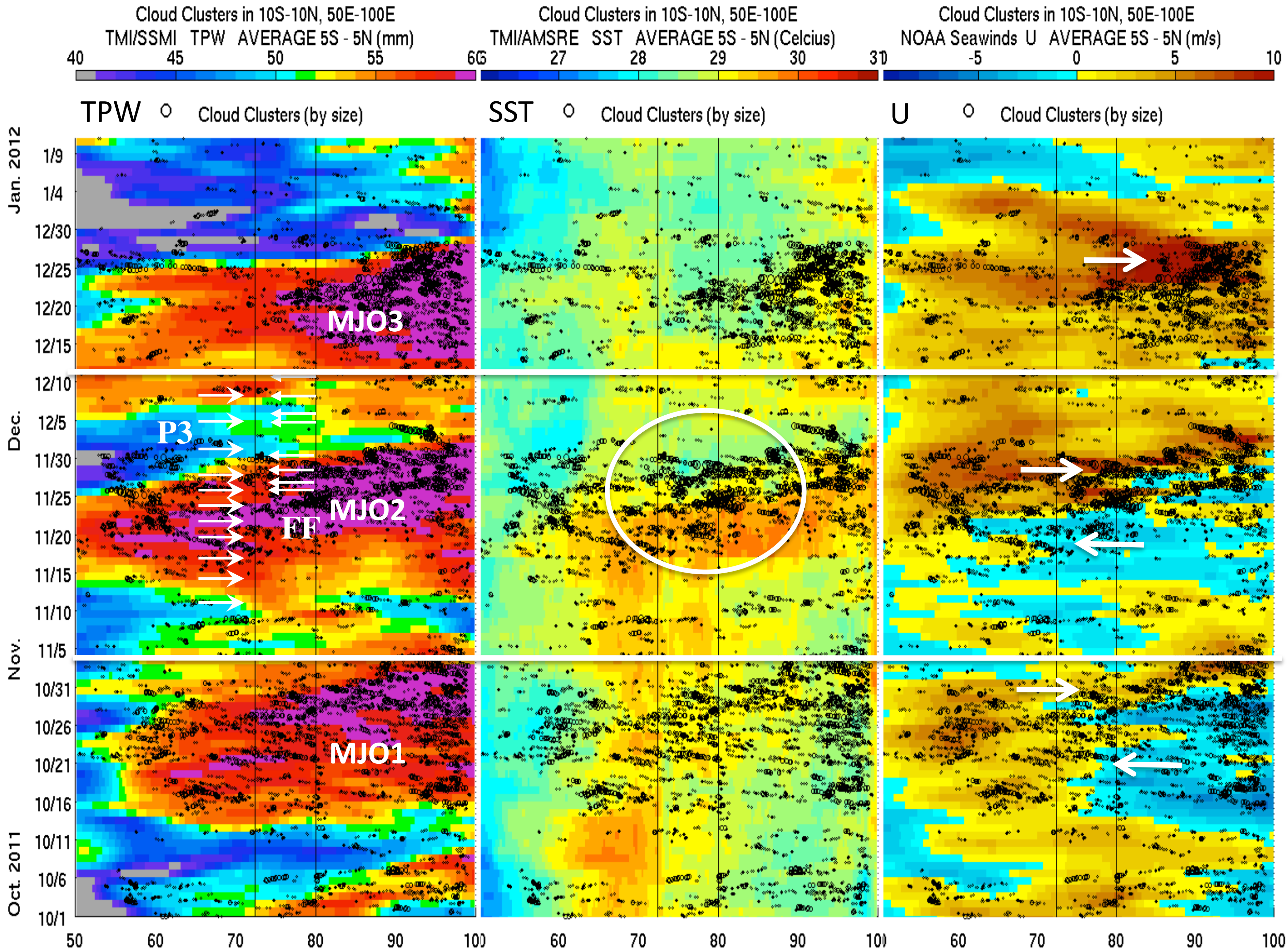

Cloud Clusters in 10S-10N, 50E-100E
TMI/SSMI TPW AVERAGE 5S - 5N (mm)
40 45 50 55 60
Cloud Clusters in 10S-10N, 50E-100E
TMI/AMSRE SST AVERAGE 5S - 5N (Celcius)
26 27 28 29 30 31
Cloud Clusters in 10S-10N, 50E-100E
NOAA Seawinds U AVERAGE 5S - 5N (m/s)
-10 -5 0 5 10
TPW Cloud Clusters (by size)
SST Cloud Clusters (by size)
U Cloud Clusters (by size)
Jan. 2012
Dec.
Nov.
Oct. 2011
1/9
1/4
12/30
12/25
12/20
12/15
12/10
12/5
11/30
11/25
11/20
11/15
11/10
11/5
10/31
10/26
10/21
10/16
10/11
10/6
10/1
MJO3
MJO2
MJO1
P3
FF
50 60 70 80 90 100

NOPP P-3:

- 12 flights (10 science + 2 test/calc)
- sampling all three MJO phases

French Falcon:

- 13 flights
- sampling active-suppressed MJO phases

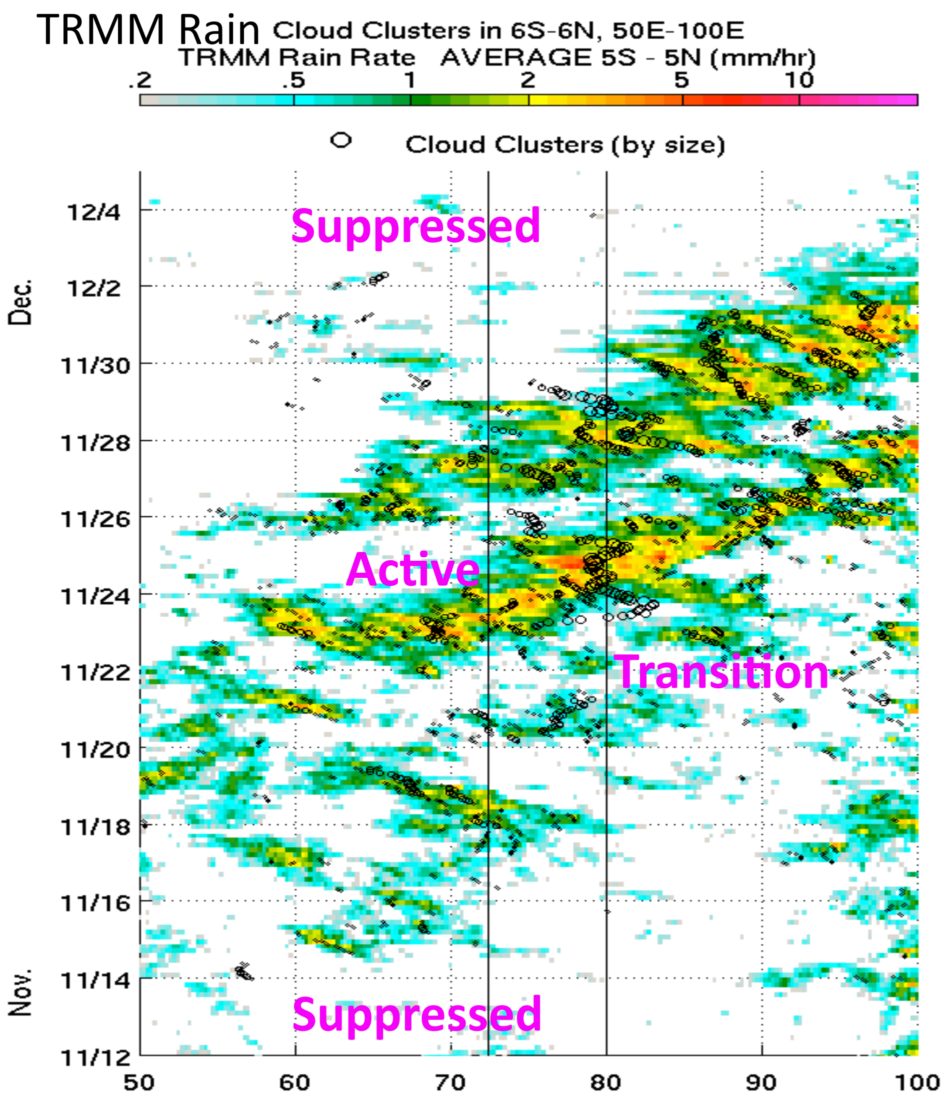

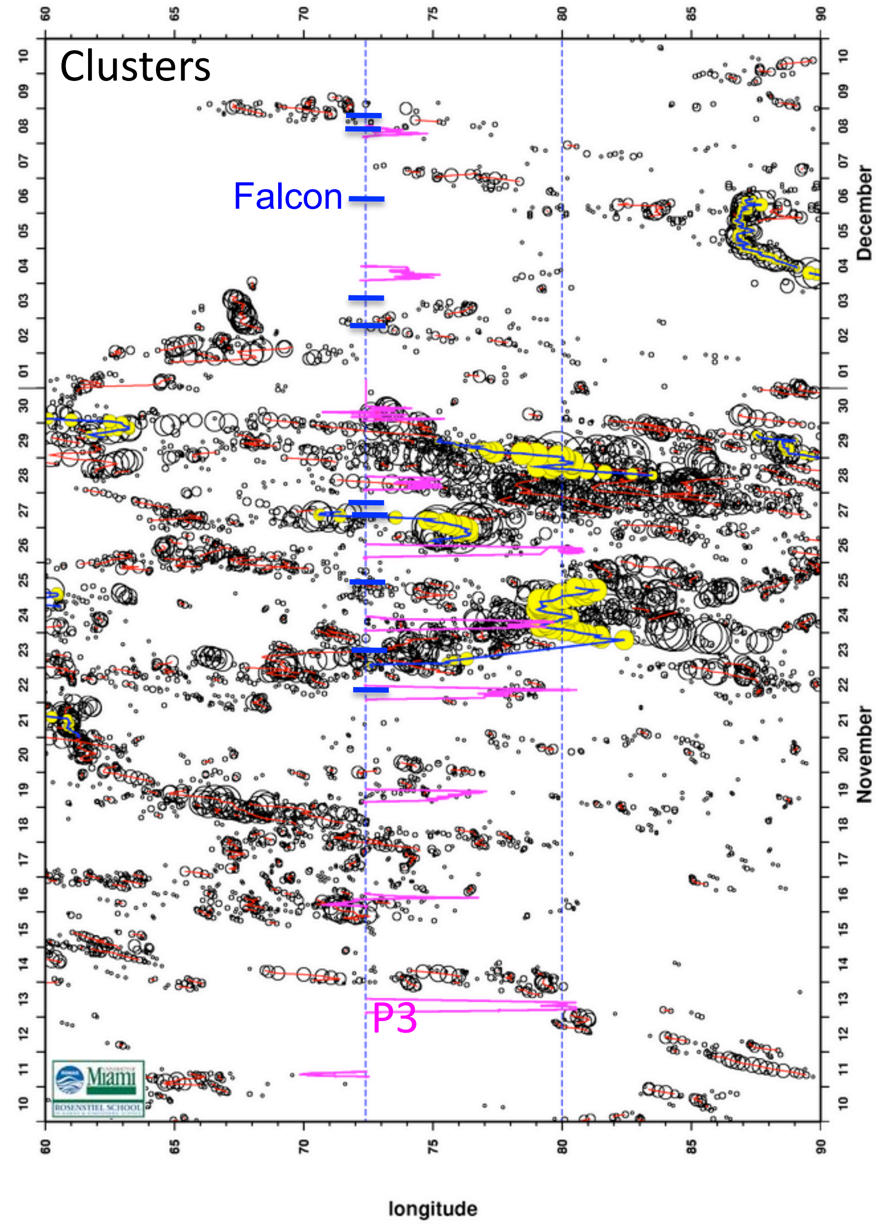

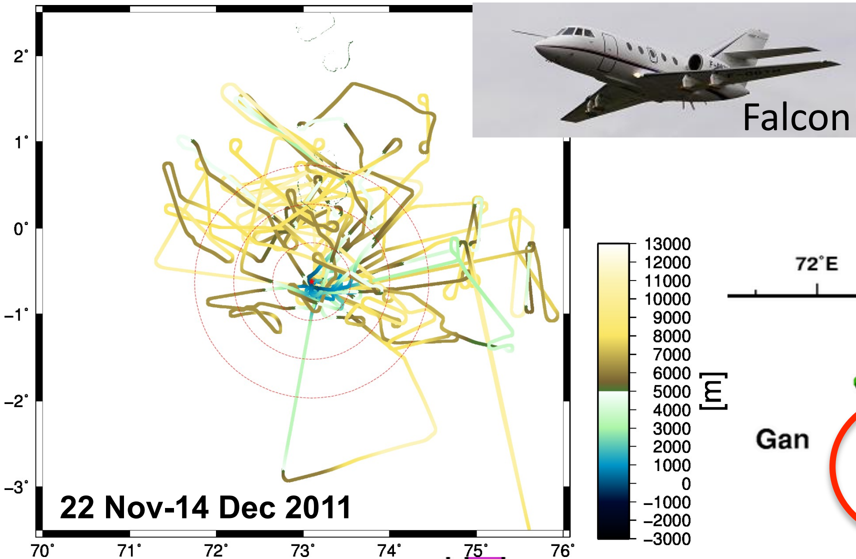

French Falcon (13 flights)

Objectives:

- Cloud structure
- Microphysical properties

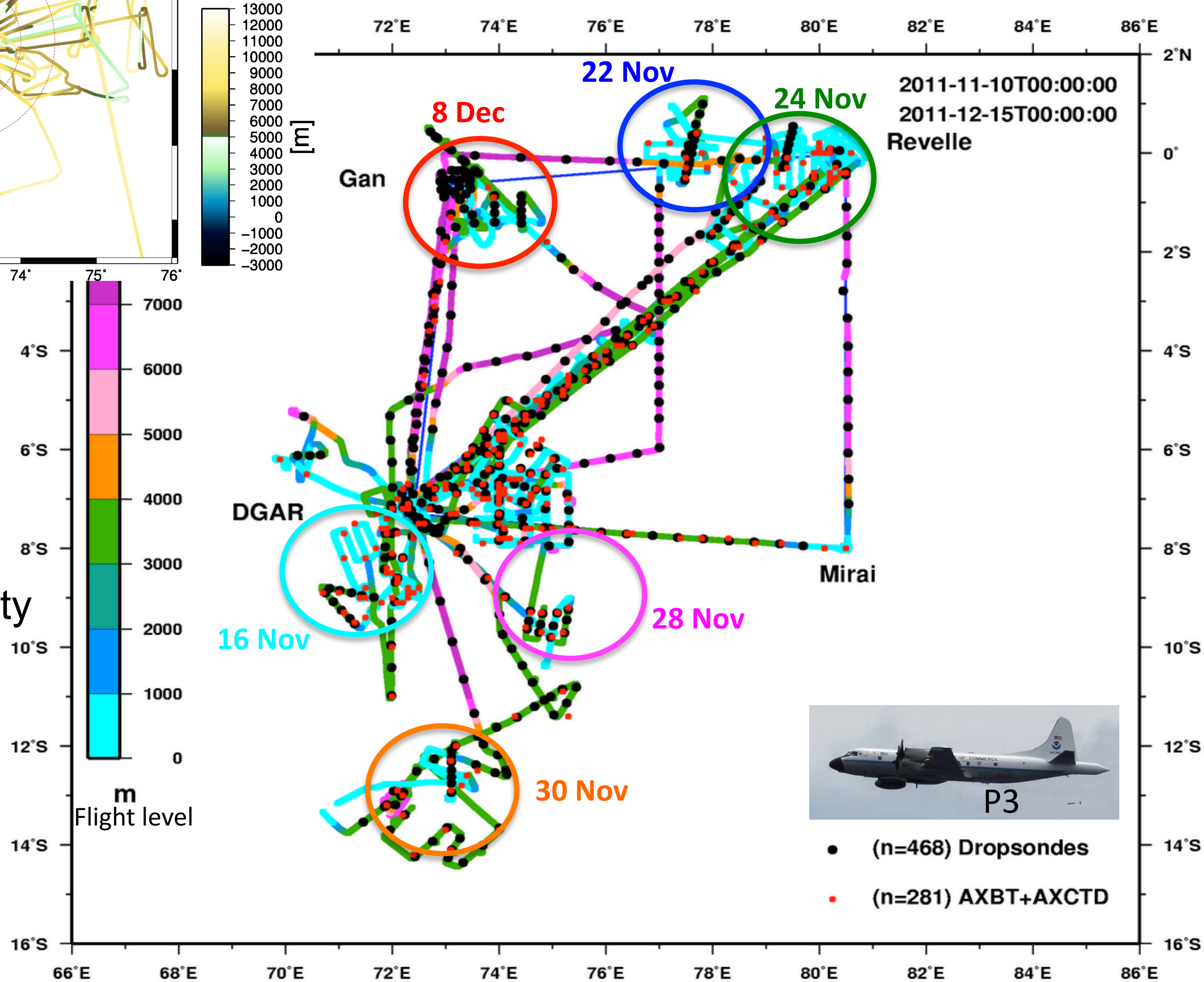

NOAA P-3 (12 flights)

Objectives:

- Convective structure
- Water vapor variability
- Air-sea fluxes

Double ITCZ (20 November 2011)

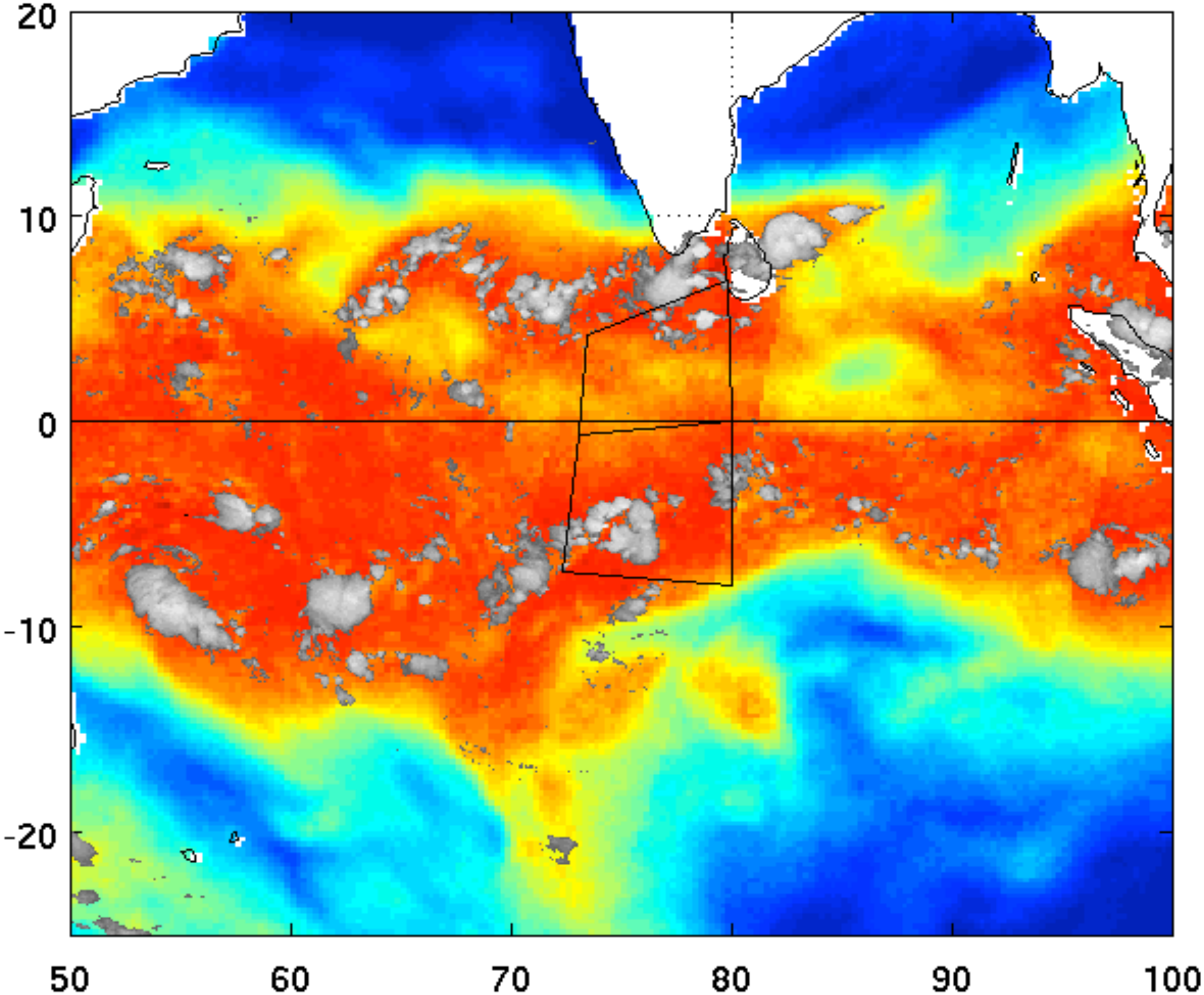

Transition to Equatorial Convection (22 November 2011)

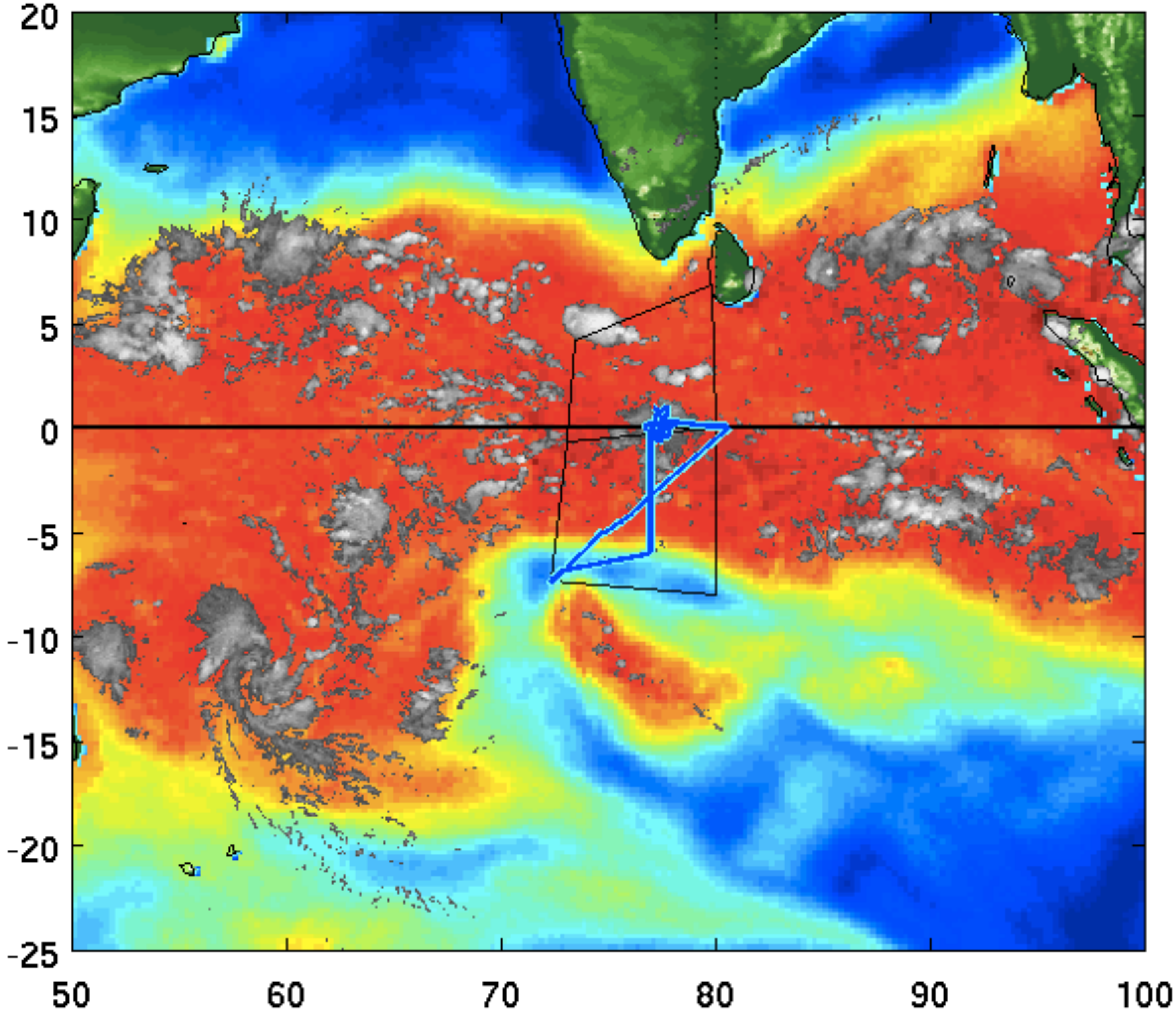

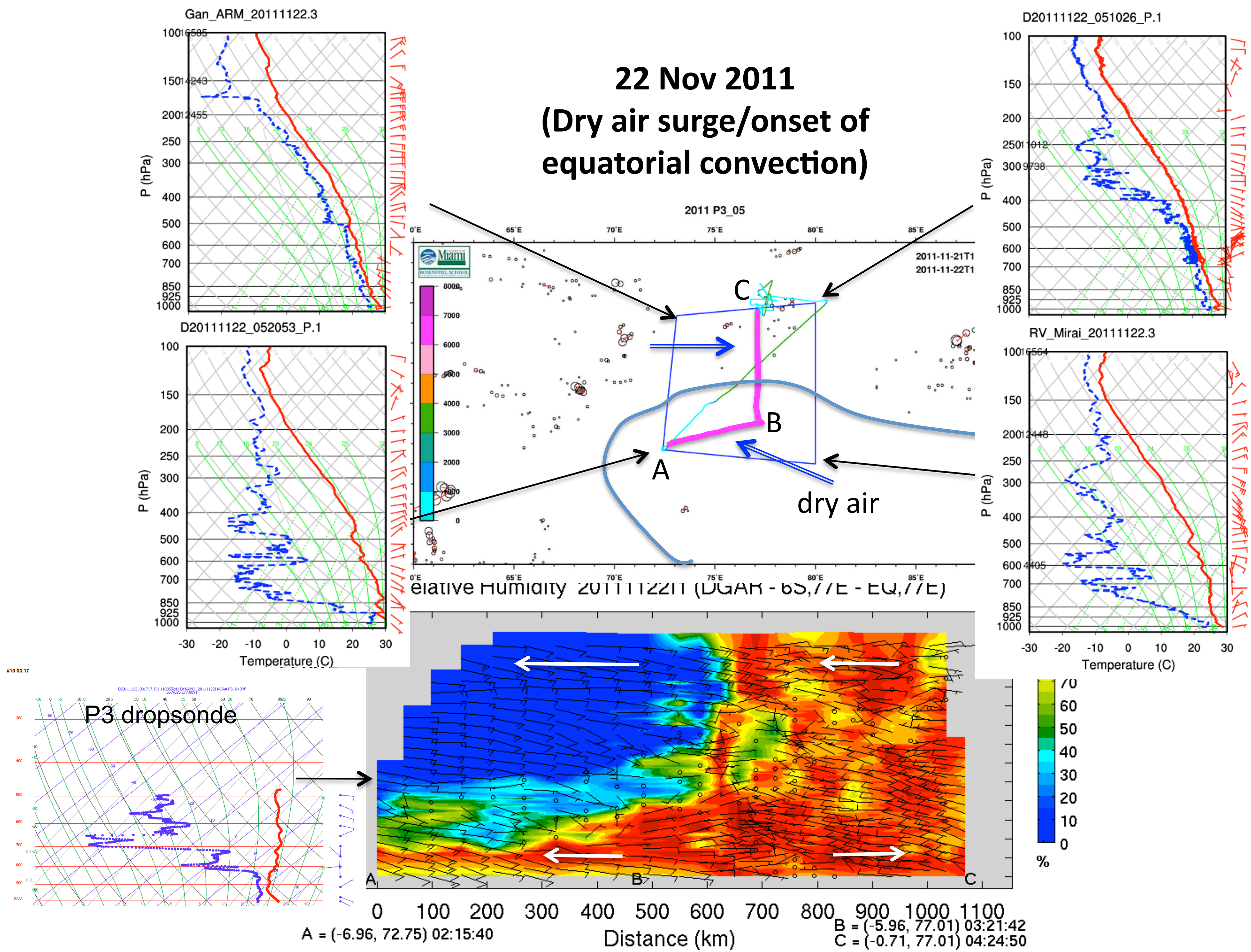
22 Nov 2011
(Dry air surge/onset of equatorial convection)
Gan_ARM_20111122.3
D20111122_052053_P.1
D20111122_051026_P.1
RV_Mirai_20111122.3
P (hPa)
Temperature (C)
2011 P3_05
2011-11-21T1
2011-11-22T1
C
B
A
dry air
P3 dropsonde
elative Humidity 20111122h (DGAR - 6S,77E - EQ,77E)
Distance (km)
A = (-6.96, 72.75) 02:15:40
B = (-5.96, 77.01) 03:21:42
C = (-0.71, 77.01) 04:24:50
%

Active Phase (24 November 2011)

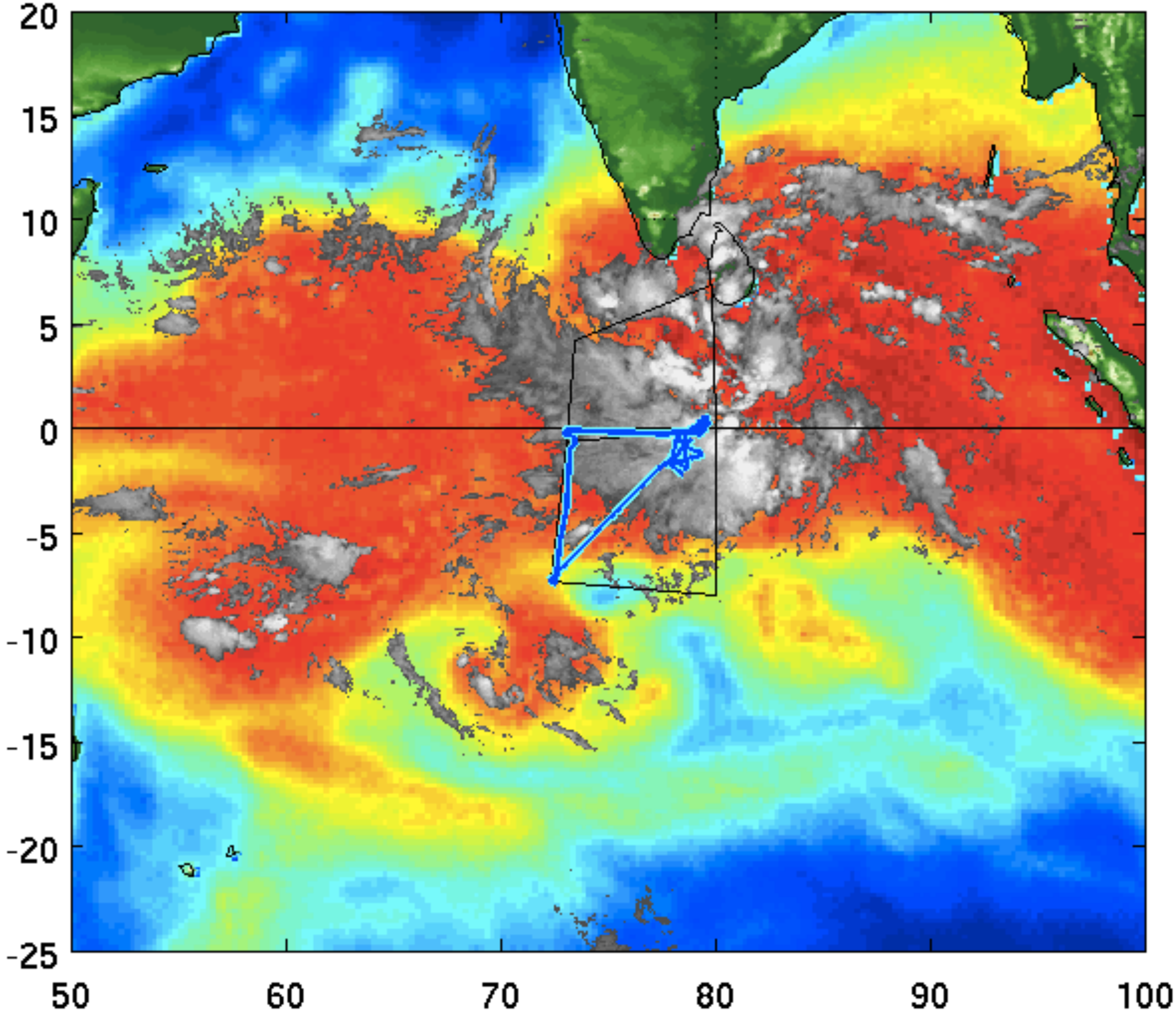

NOAA P-3 Dropsonde Equatorial Cross Section 0810-0934 UTC 24 Nov 2011

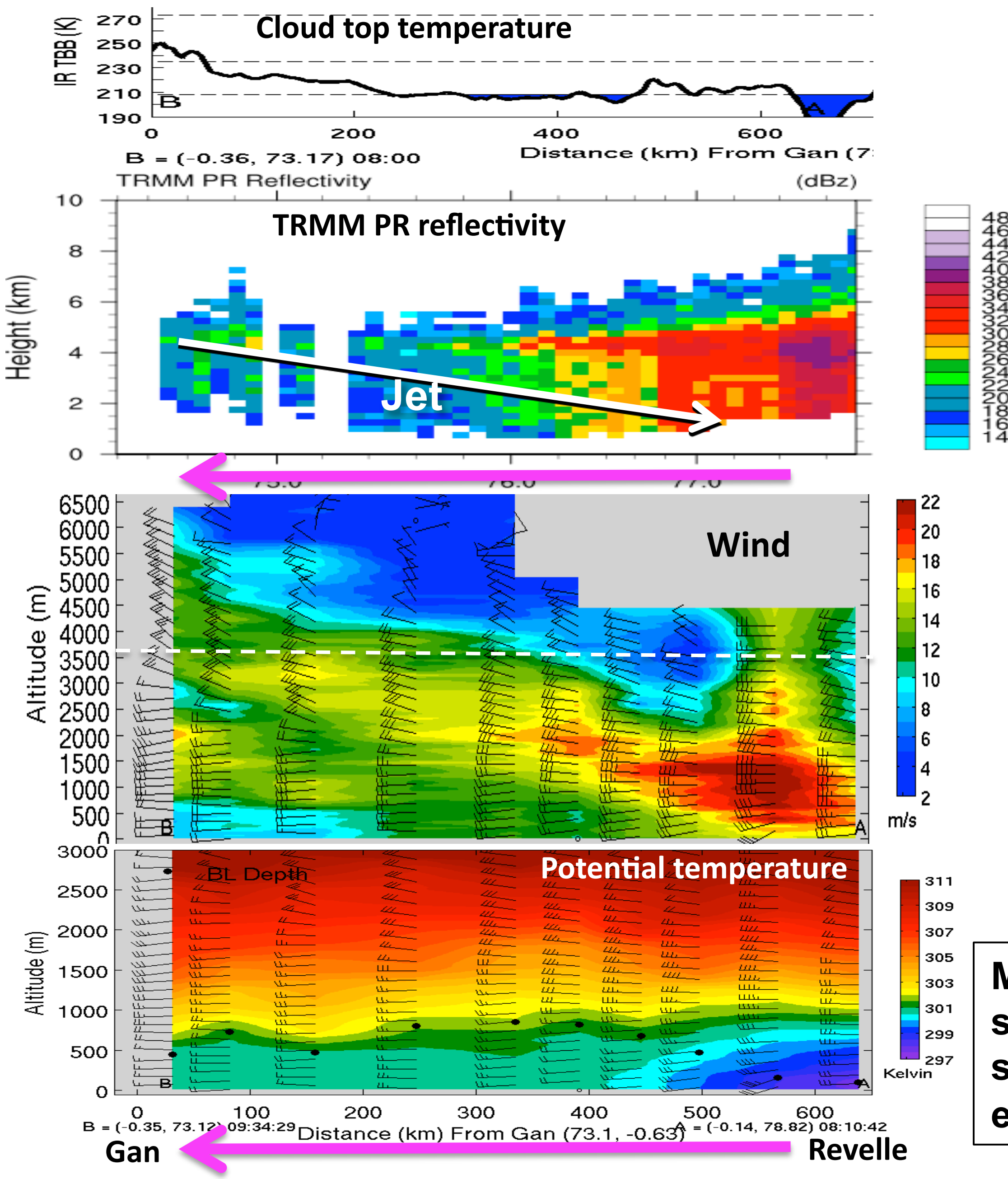

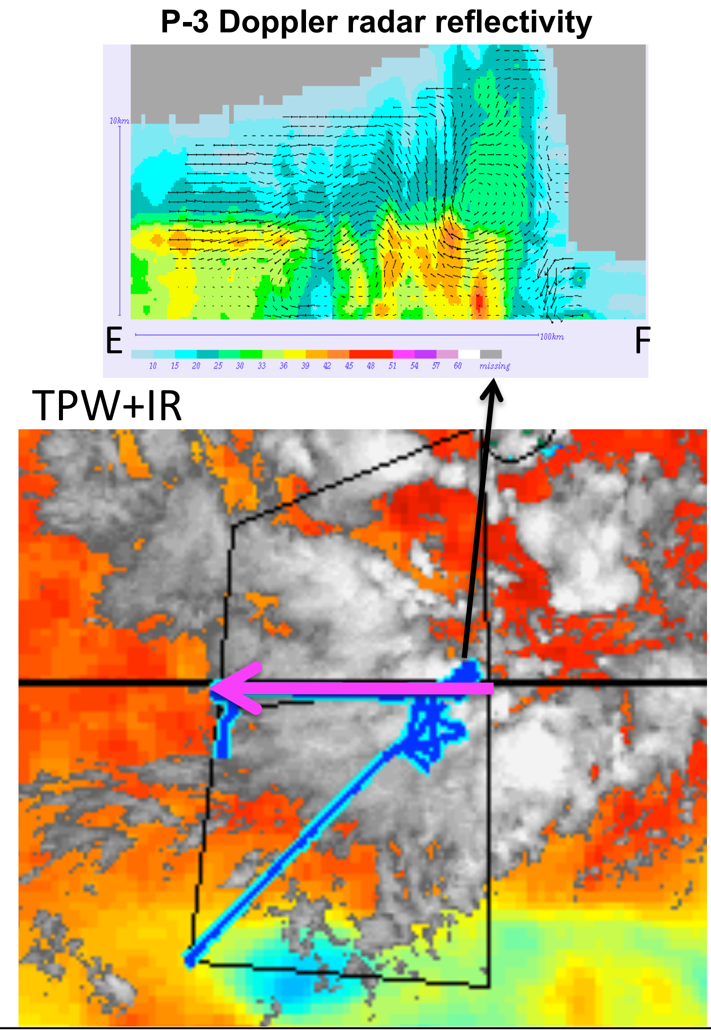

Momentum transport by convective systems in MJO from mid-level to surface (Houze et al. 2000, Mechem et al. 2003)

Suppressed (Nov 13)/Low winds

Active (Nov 26)/High winds

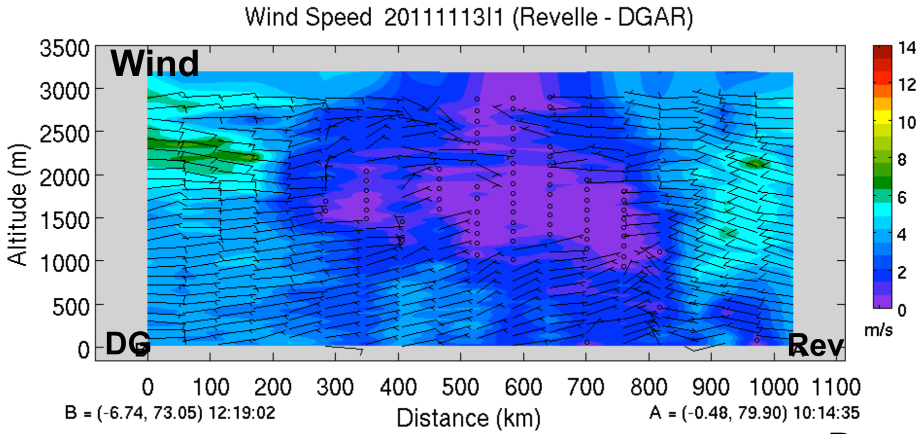

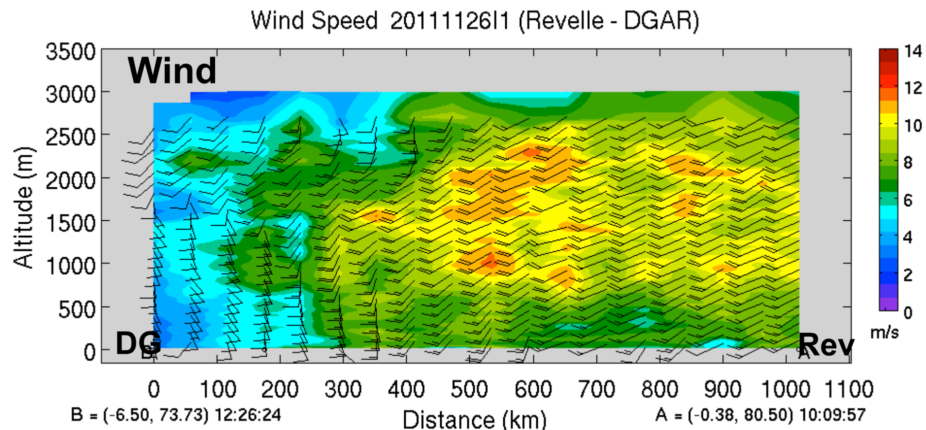

Dropsondes

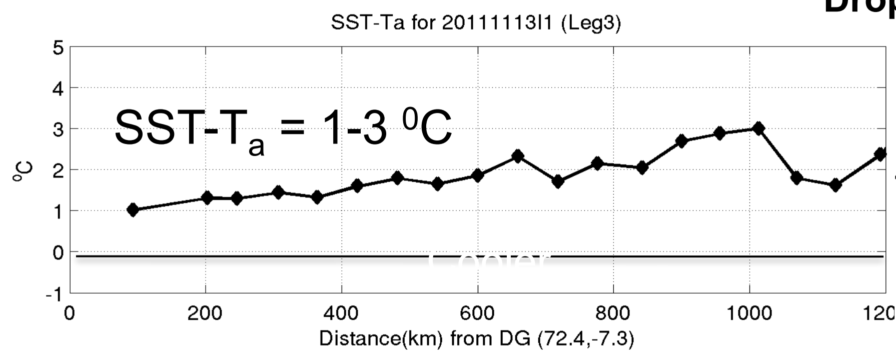

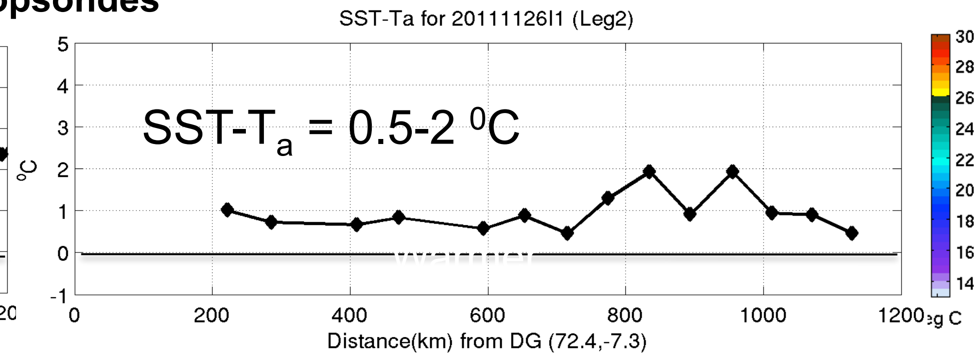

AXBTs

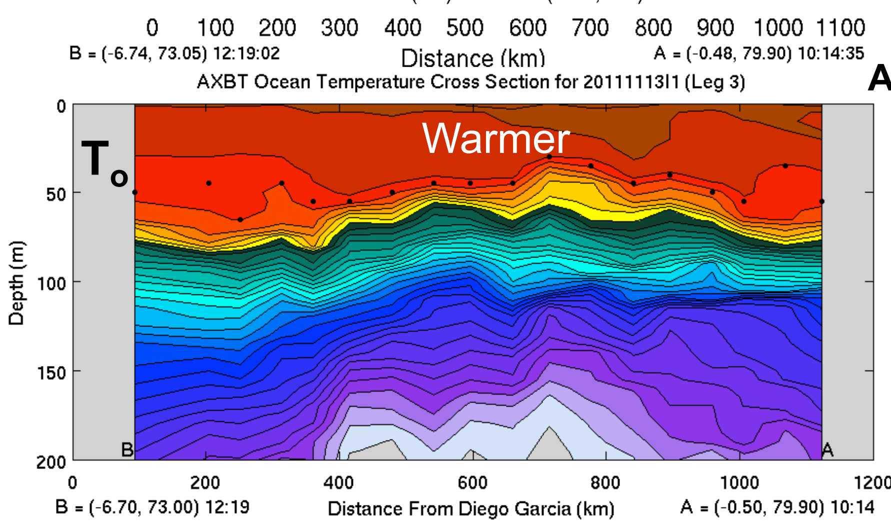

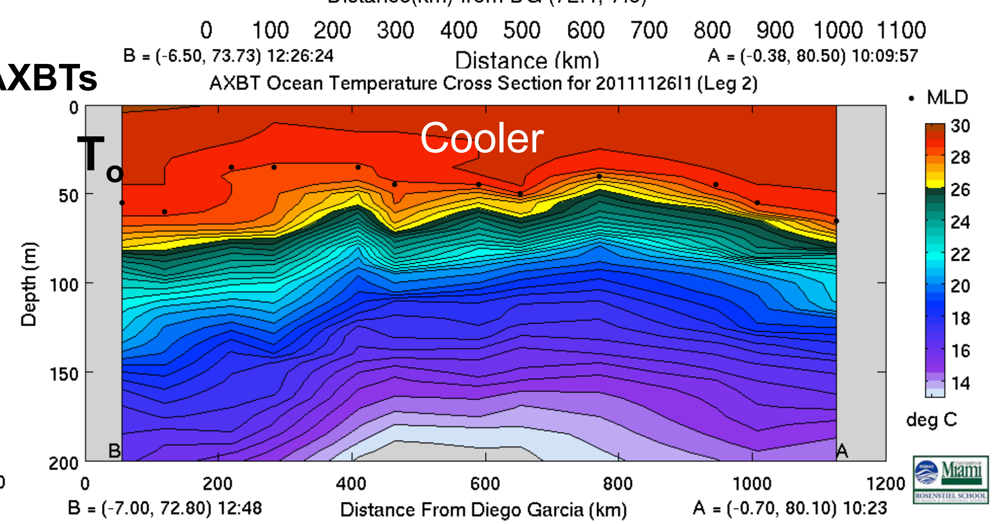

Suppressed Phase (08 December 2011)

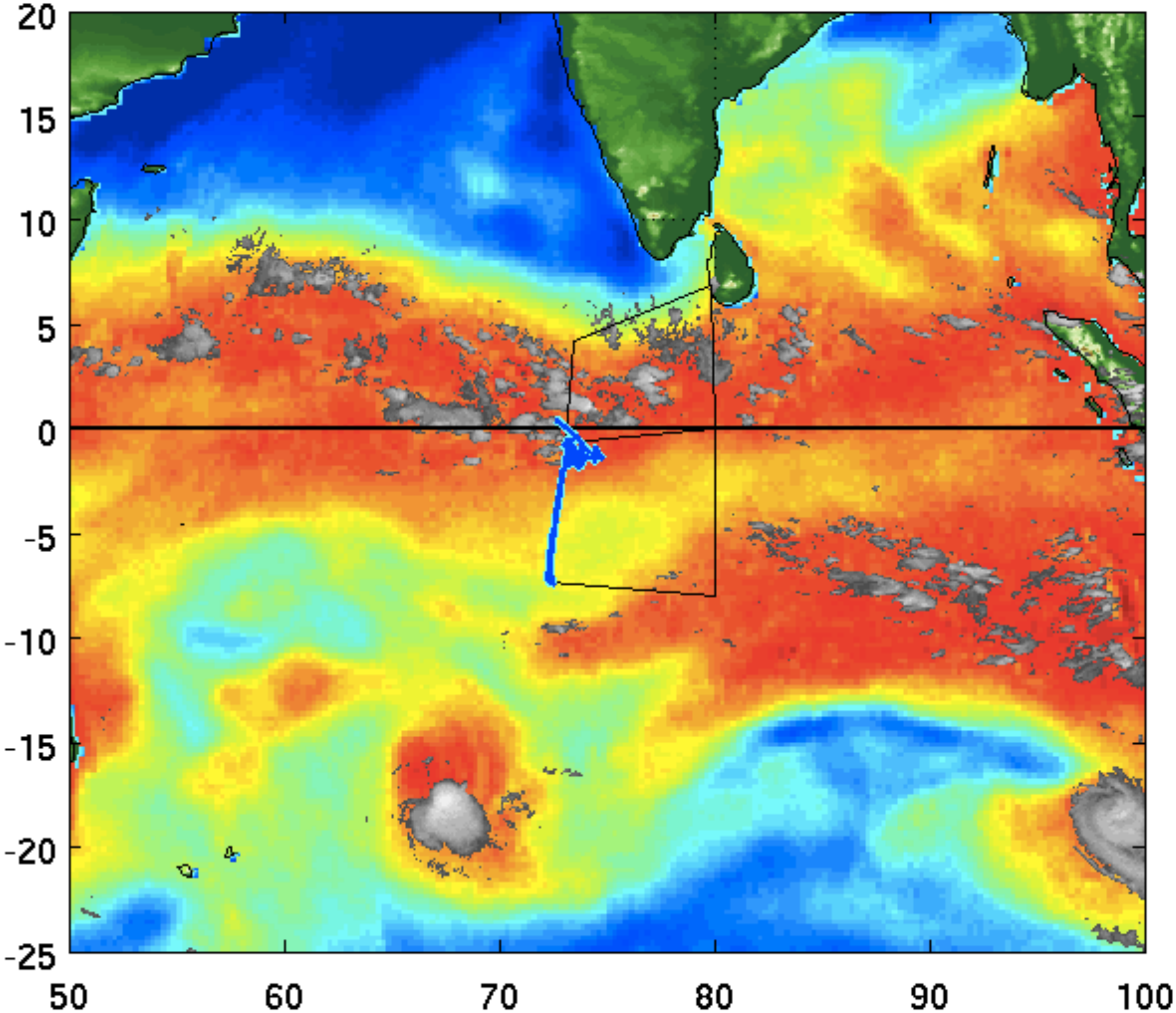

Multi-Radar Observations of Convective Systems in DYNAMO

(P3 C-band and Falcon W-band Doppler radar 0750-0759 UTC 8 December 2011)

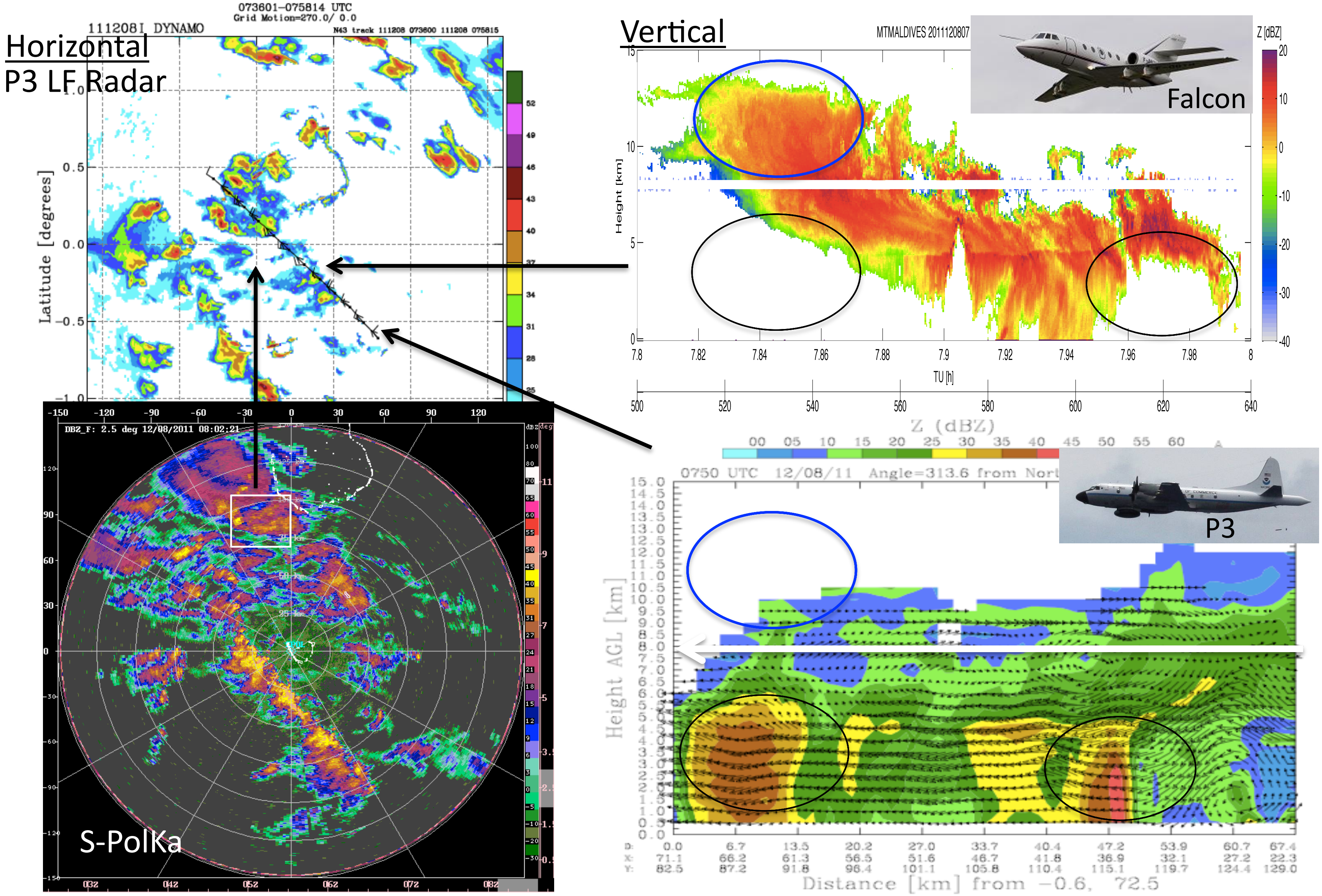

Falcon Radar Retrieved Ice Microphysical Properties

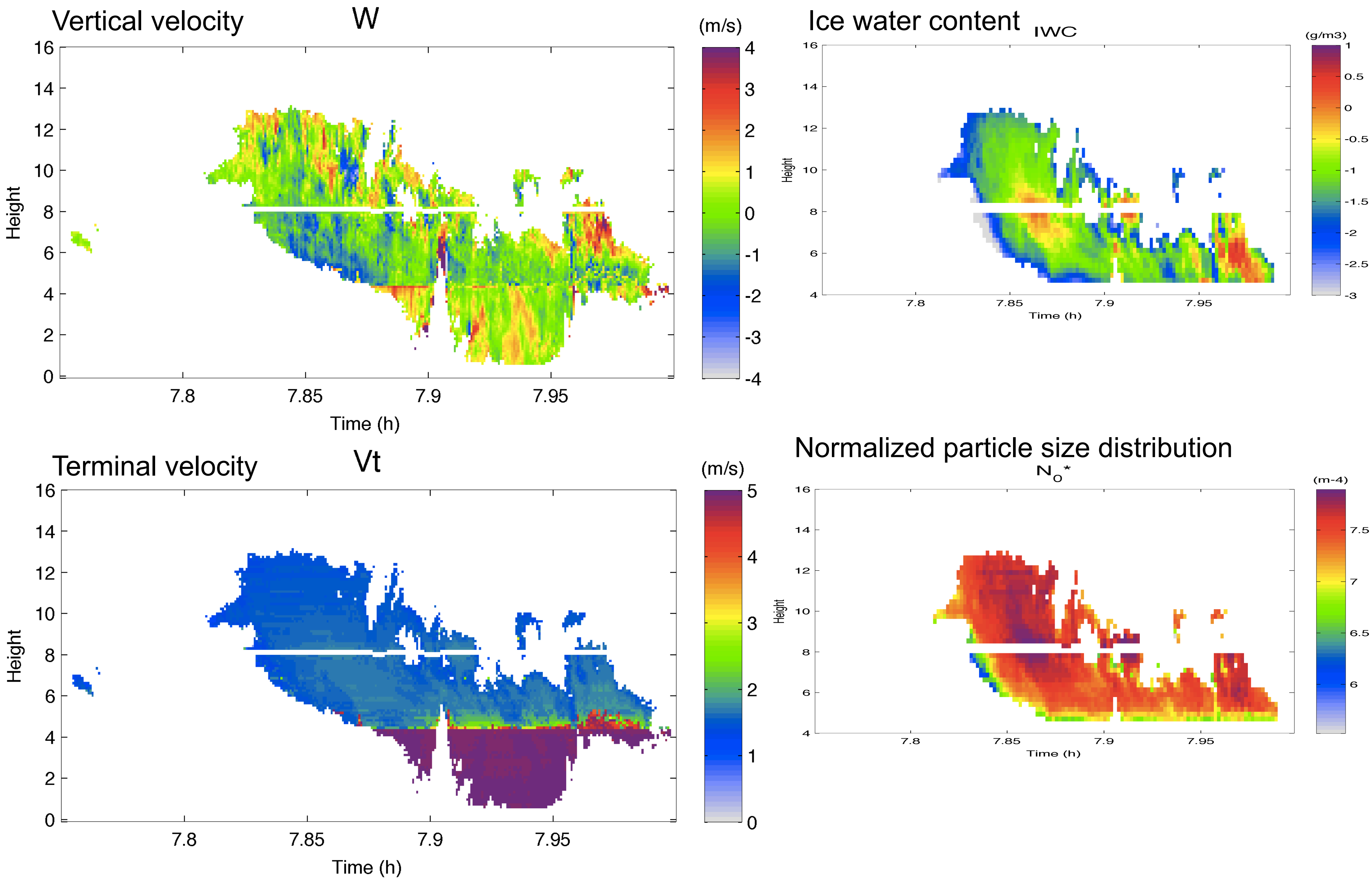

Convective Cold Pools Using P-3 Dropsondes and AXBTs

(Savarin et al., Poster: A13A-0211)

Cold pool soundings

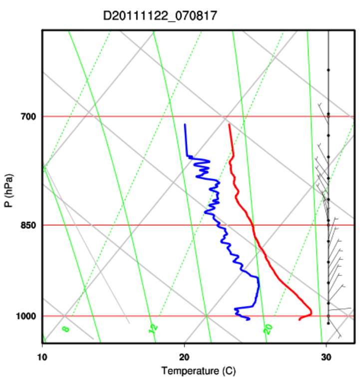

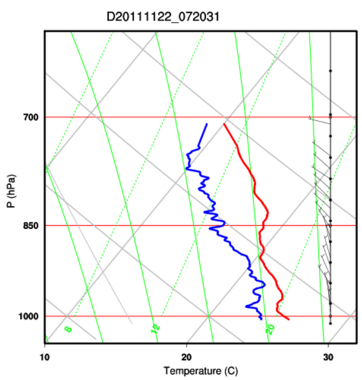

Environmental

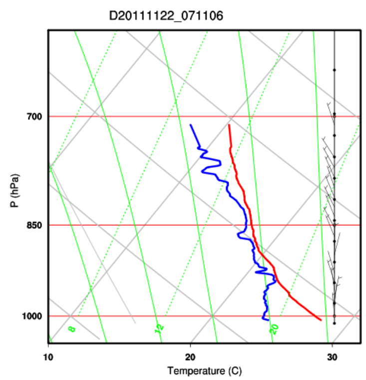

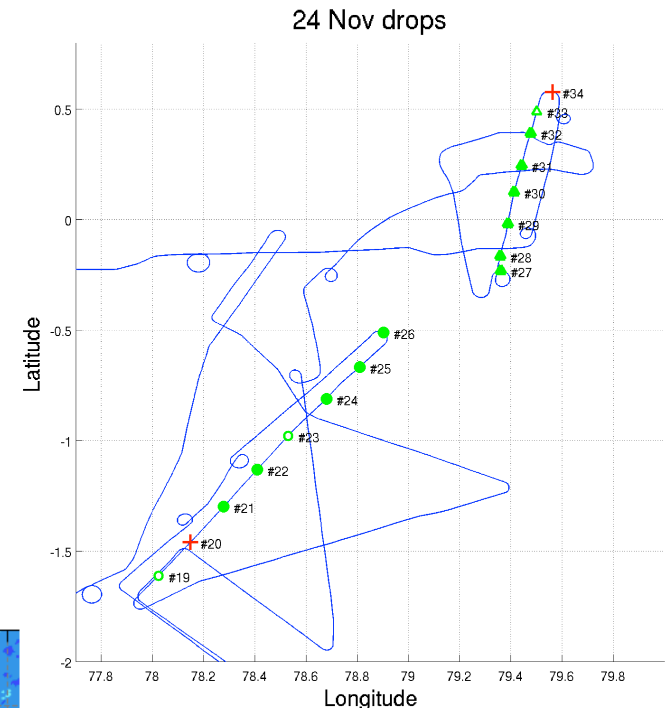

Cold pool depth (negative buoyancy layer)

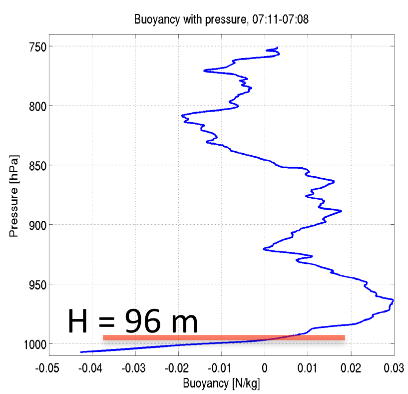

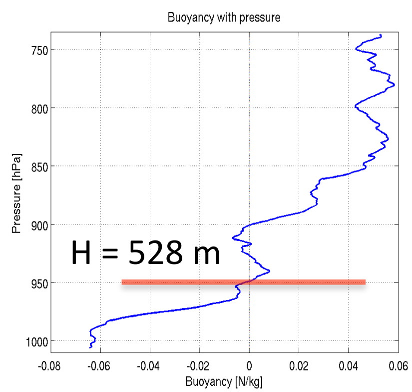

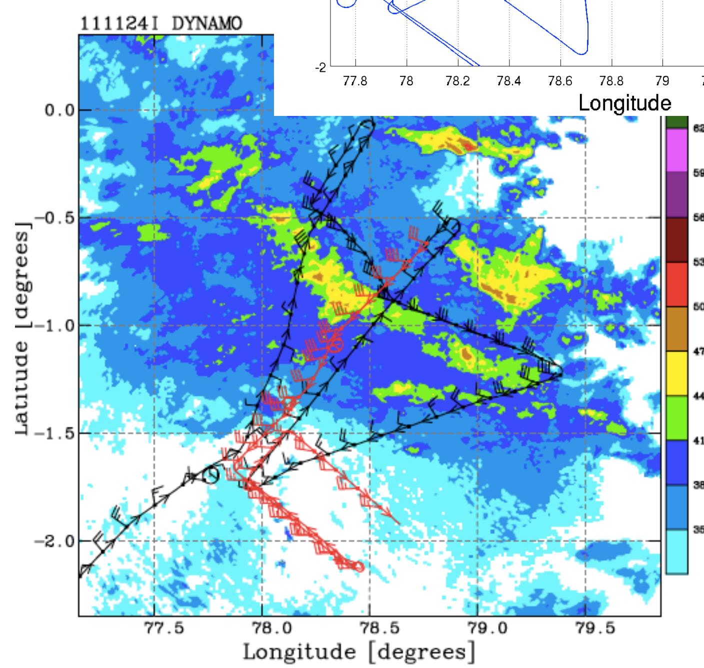

Convective Cold Pools and Boundary Layer Recovery

- Buoyancy: $$B = g\left[\frac{\theta + \overline{\theta}}{\overline{\theta}} + 0.61\left(q - \overline{q}\right)\right]$$

- Cold pool intensity: $$C = \sqrt{\frac{2}{\overline{\rho(z=0)}}\int_0^H \overline{\rho} B\,dz}$$

- COARE 3.1 sensible and latent heat fluxes:

$$LH = L_e \cdot \rho_{10} \cdot u_{10} \cdot c_q \cdot \Delta T \qquad SH = C_p \cdot \rho_{10} \cdot u_{10} \cdot c_e \cdot \Delta q$$

$$\Delta T = SST - T_{10} \qquad \Delta q = q_{sat}^{SST} - q_{10}$$

- Recovery time:
  (Jorgensen et al. 1997)

$$t_r = h \cdot \left[\frac{\Delta_z \overline{\theta} \cdot \Delta_t \langle \overline{q} \rangle - \Delta_z \overline{q} \cdot \Delta_t \langle \overline{\theta} \rangle}{\overline{LH}\big|_{sfc} \Delta_z \overline{\theta} - \overline{SH}\big|_{sfc} \Delta_z \overline{q}}\right]$$

h = BL height

$$\Delta_t \langle \overline{q} \rangle = \overline{q}_{final} - \overline{q}_{initial}$$

$$\Delta_t \langle \overline{\theta} \rangle = \overline{\theta}_{final} - \overline{\theta}_{initial}$$

$$\Delta_z \overline{q} = \frac{q(h) - \overline{q}^{(h-100m)}}{\Delta_z} \qquad \Delta_z \overline{\theta} = \frac{\theta(h) - \overline{\theta}^{(h-100m)}}{\Delta_z}$$

Convective Systems in Transition (Nov 22), Active (Nov 24), Suppressed (Dec 8) MJO Phases

Cold Pool/Boundary Layer Recovery

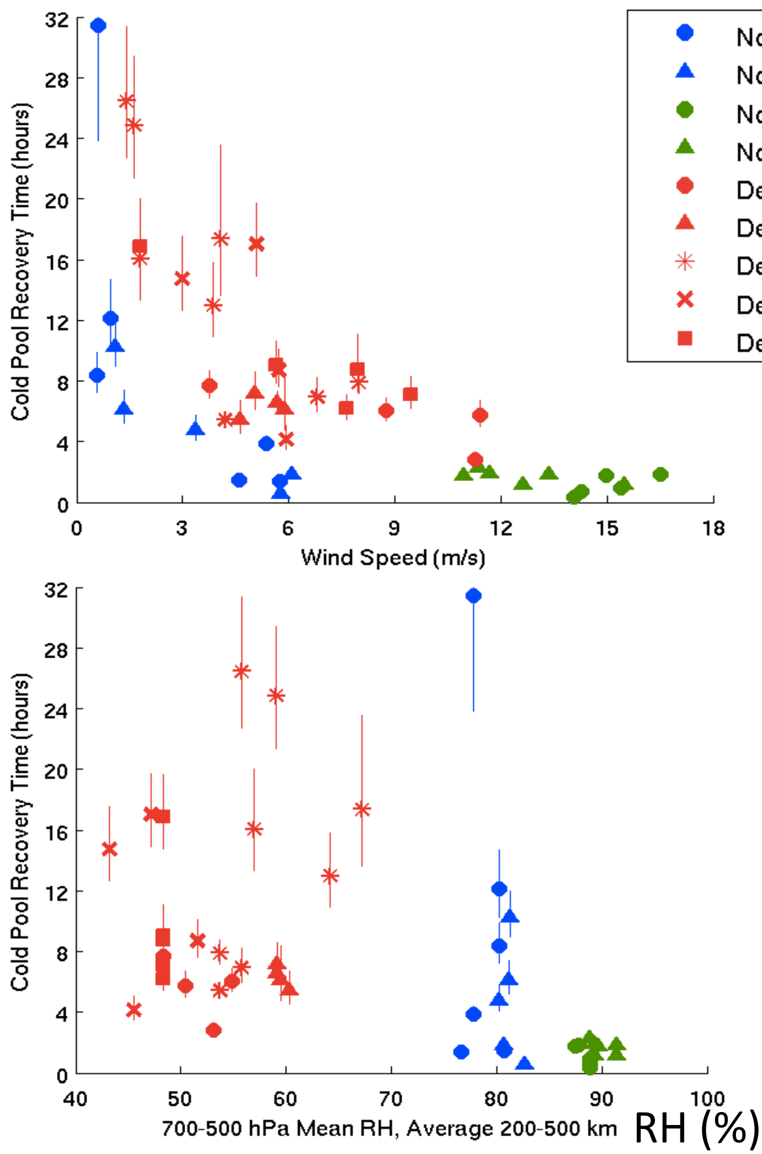

Air-Sea Fluxes

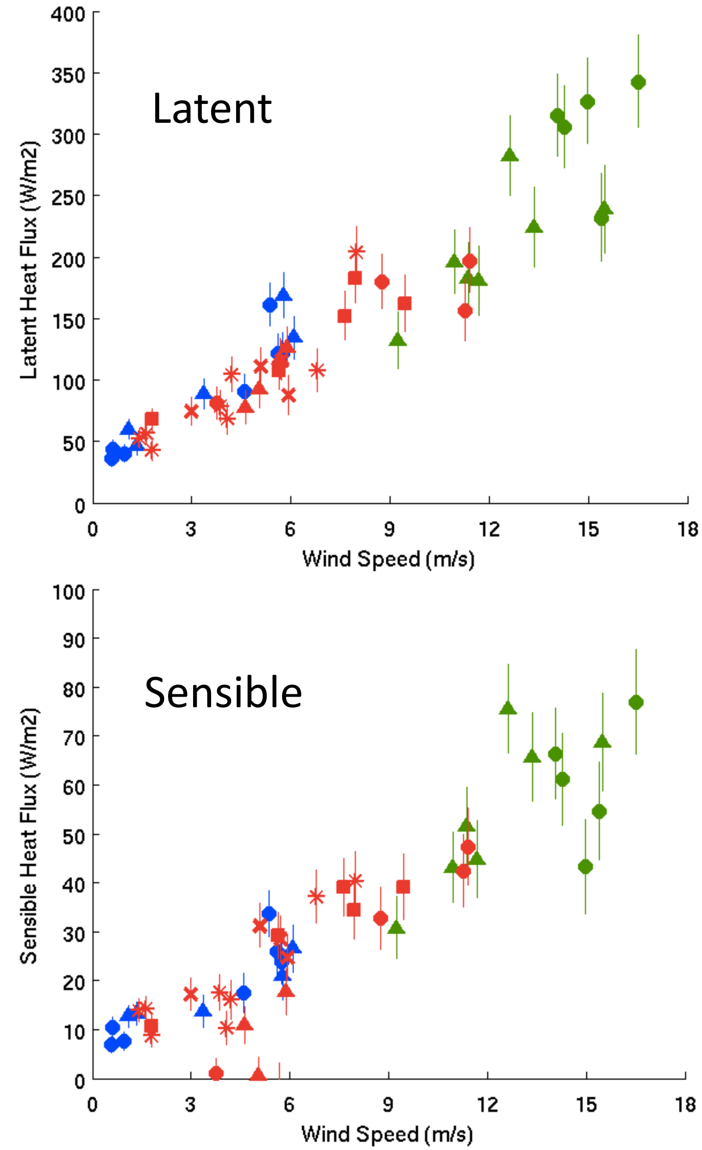

(see Jorgensen et al., and Guy et al., Poster: A13A-0210)

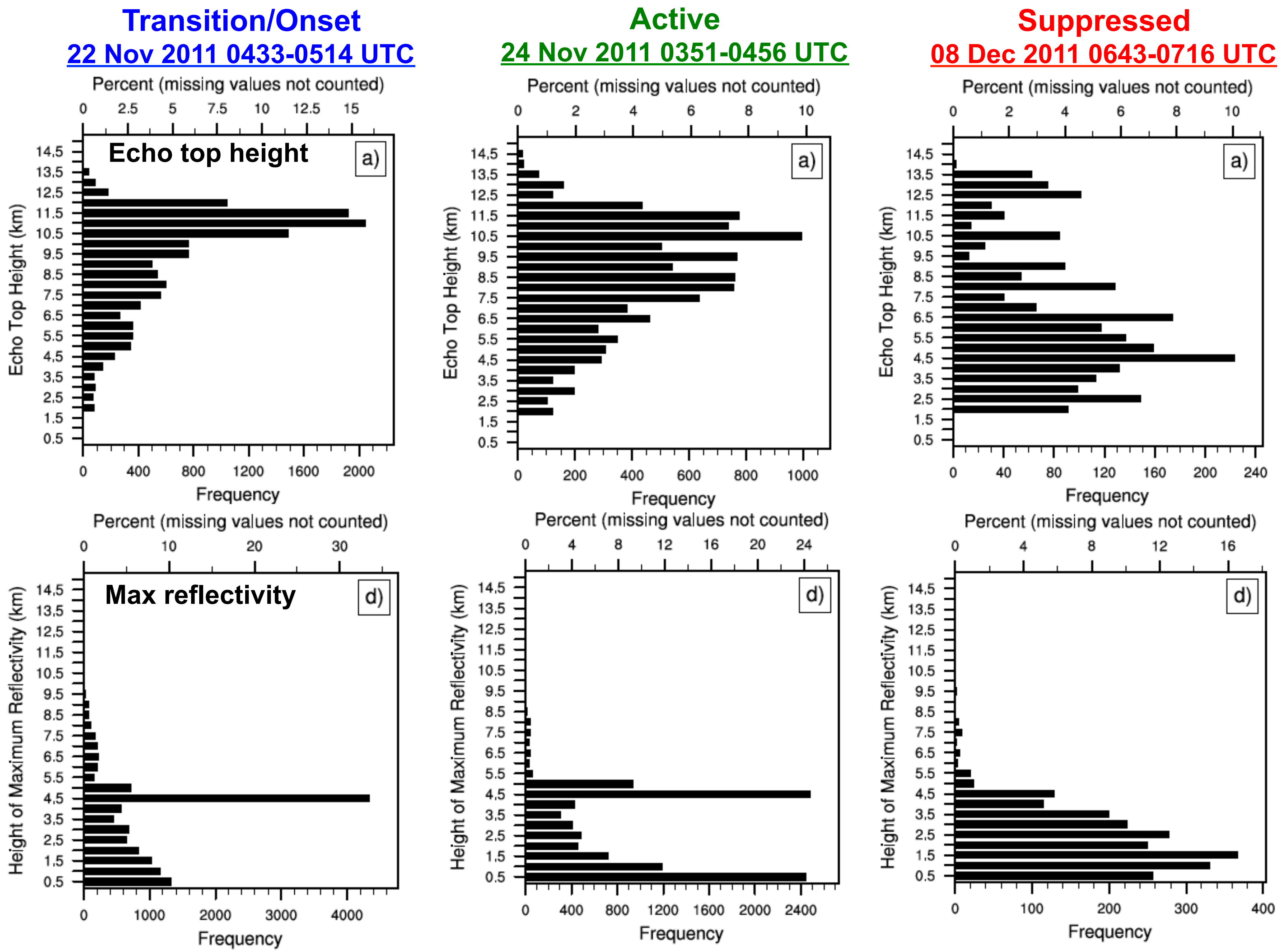

SUMMARY

- Aircraft sampling in suppressed, transition, and active phases of MJO provided observations of both convection and the large-scale atmospheric moisture, temperature, wind, and upper ocean observations using dropsonde and AXBT data

- P-3 and Falcon multi-radar (C-band, W-band) provide unique observation of full 3-D structure of convective cloud systems

- Dropsonde data provided in-situ observation of mid-low level jet associated with large convective systems, which may contribute downward westerly momentum transport in MJO

- Convective cold pools are stronger and deeper in the suppressed than active phase of MJO, which may be a result of drier environment. Both low winds and low mid-level moisture contribute to slower boundary layer recovery in the suppressed phase of MJO.